Structural Engineering and Mechanics, Vol.1, No.1 (1993) 61-74
DOI: http://dx.doi.org/10.12989/sem.1993.1.1.061

Three dimensional transition solid elements for adaptive mesh gradation

Chang-Koon Choi† and Nam-Ho Lee‡

Department of Civil Engineering, Korea Advanced Institute of Science and Technology, Taejon 305-701, Korea

Abstract. A new three-dimensional transition solid element was presented for the automated three-dimensional adaptive h-refinement or the local mesh refinement where the steep stress gradient exists. The proposed transition element was established by adding variable nodes(element nodes) to basic 8-node for an effective connection between the refined region and the coarse region with minimum degrees of freedom possible. To be consistent in accuracy with 8-node solid element with nonconforming modes, this transition element was also improved through the addition of the modified nonconforming modes. Numerical examples show that the performance of the element and the applicability to 3D adaptations are satisfactory.

Key words: adaptation; basic node; constraint; different layer; hexahedron; irregular node; mesh gradation; nonconforming modes; regular node; solid transition element; variable-node.

1. Introduction

The eight-node hexahedron solid element has been frequently used in the three dimensional structural analysis due to its simplicity and easy availability. This element can be easily found in most of element libraries of structural analysis computer programs and the modeling of complicated 3D-structure by this element is relatively easier than by other brick elements. Furthermore, when the behavior of element is improved by the addition of nonconforming modes, structural analysis by this element provides reliable results with high accuracy. Therefore, many massive structures, such as the internal shield wall of nuclear reactor building have been modeled and analyzed by using this element. However, when a complicated structure needs to be gradually refined locally and reanalyzed due to the existence of steep stress gradient and/or the singularity due to the concentrated local load, the overall mesh should be reconstructed to be consistent with the local stress gradient. For such mesh gradation, the use of eight-node solid elements often leads either to meshes with highly distorted elements or to meshes with too many degrees-of-freedom which may exceed the economical limit of computation.

For the local mesh refinement, the adaptive h-refinement has been intensively used, in particular for two-dimensional elastic problems. For three-dimensional problems, however, only a few initial works have been reported in the current literature(Devloo 1991, Chang and

† Professor
‡ Research Assistant

Choi 1992). In 3D adpative mesh refinement, Devloo used the enforced compatibility between the refined region and the unrefined region through constraint conditions applied during the formulation of 3D solid element stiffness while Chang used the distorted solid elements in his mesh refinement. However, in addition to the deficiency of the element itself, i.e. too stiff against flexure, applying too many displacement constraints and/or using the highly distorted mesh may cause some drawbacks in obtaining reliable analysis results irrespective of the refinement strategy. Furthermore, the use of such constraints requires a lot of information about element's neighbors while formulating its stiffness matrix.

This paper presents a new transition element with a variable number of nodes that can be effectively used in the adaptive mesh refinement by connecting the locally refined mesh to the existing coarse mesh through a minimum mesh modification in transition zone. The behavior of this variable-node element has been also improved through addition of modified nonconforming modes to obtain more accurate solutions. This new transition elements enable us to automatically refine any element without simultaneously modifying the adjacent elements to provide connections for any new nodes generated by subdivision of the element. Also, the aforementioned problems due to the mesh distortion can be relieved since this type of transition elements can keep the square or cubic shapes as required. Some numerical examples are presented to verify the behavior of the proposed transition element and to demonstrate the applicability to 3D adaptive mesh refinement.

This paper is the first part of the study on the use of transition element for adaptive mesh gradation, emphasizing the development of the transition element for mesh gradation. It will be followed by the second paper which emphasizes the application of the transition element into the adaptive mesh refinement scheme.

2. Three-dimensional solid transition elements

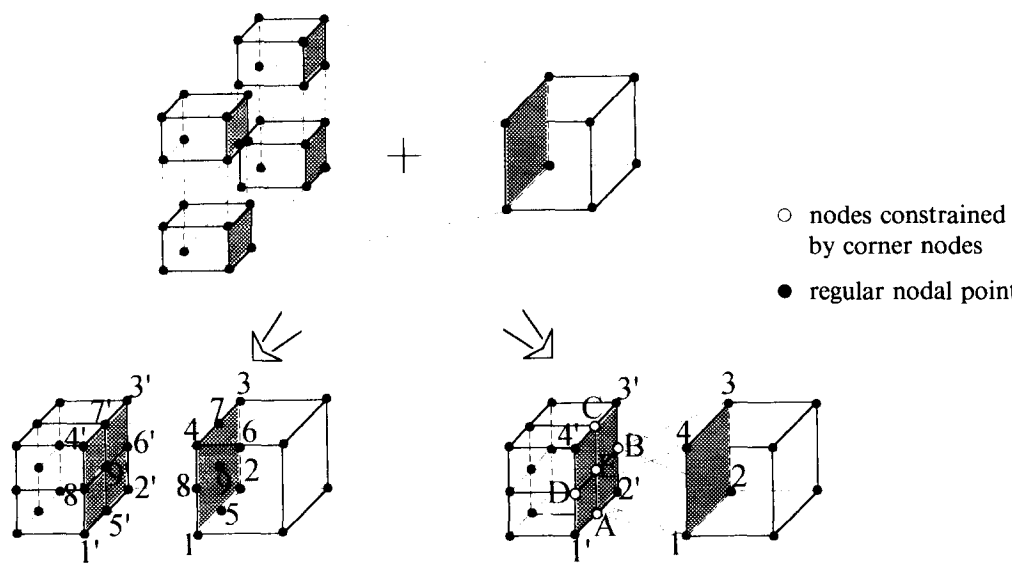

(a) introduction of 3D transition element (b) use of constraints

Fig. 1 Connection of different mesh layers

Fig.1 shows an example of the use of the transition element in comparison with the use of constraints for mesh gradation. Fig.1(a) shows an easy connection between a variable-node element(13-node element) and four subdivided eight-node elements whereas the behavior of five irregular nodes(nodes A, B, C, D, and E) should be constrained by those of regular nodes (nodes 1, 2, 3, and 4) as shown in Fig.1(b). Here the irregular node is defined as a node which is not directly connected to physical(regular) nodes.

In the element libraries of most computer programs for structural analysis, two types of three-dimensional variable-node solid elements as shown in Fig.2 are frequently available. However, these elements were not developed particularly for direct application to the three-dimensional h-refinement and when used as a transition element in h-refinement, there are two limitations: (*i*) The first limitation is associated with the treatment of the irregular nodes to be located at the centroids of faces. The first element(Fig. 2(a)) which has variable number of nodes from 8 to 20 do not have a node at the centroid of the face to be connect by irregular nodes generated in the subdivided region and the second element(Fig. 2(b)) which is established by adding upto 6 variable nodes to the 21-node element generate unnecessarily more degrees-of freedom since all the nodes at mid-points of 12 edges of the hexahedron should be defined even if only one or two irregular nodes at the centroid of faces are actually needed; (*ii*) The eight-node hexahedron element generally do not provide reasonably accurate solution without an extensive mesh refining. Therefore, the eight-node hexahedron need to be improved for practical use. One of the effective ways to achieve such improvement is through the addition of nonconforming modes(Cook 1981, Zienkiewicz and Taylor 1989).

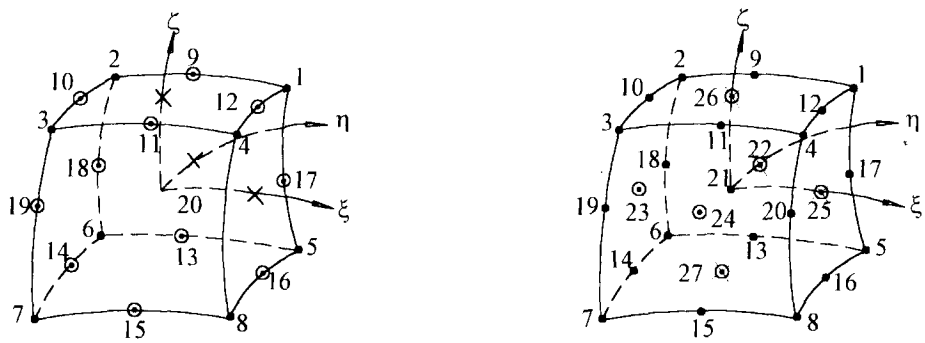

(a) Allowed mid-edge nodes to be introduced on any element edge with 8 basic corner nodes

(b) Allowed mid-face nodes to be introduced on any element face along with 21 basic nodes

⊙ variable node • basic node

Fig. 2 Two types of variable-node elements

Configuration of 3D variable-node solid transition elements

To eliminate the aforementioned first shortcoming of the hexahedron, a new transition element which can be put irregular nodes as needed at any of mid-points of 12 edges, center-points of 6 faces, and a centroid of hexahedron is proposed. Based on the basic configuration and the node numbering of element, a series of new solid transition elements which have up to 27 nodes can be systematically established. Among these, 13-, 15-, 17-, 18-, 23-node elements are most frequently used in the practical problems. A brief description of the derived

shape functions for the element has been included in Appendix.

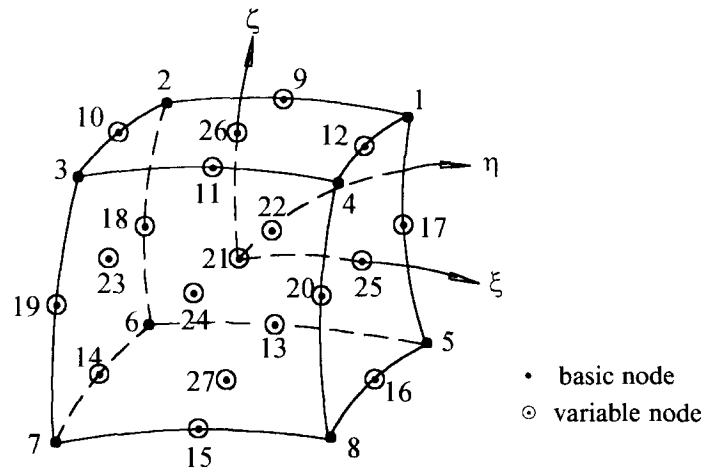

Fig. 3 Transition element with variable nodes from 8 to 27

Addition of modified nonconforming modes

To avoid shear locking and also improve the general behavior of the brick type element, the typical nonconforming modes $1-\xi^2$, $1-\eta^2$ and $1-\zeta^2$ have been added to the eight-node isoparametric solid element with great success(Cook 1981). When the conventional variable-node solid elements i.e. elements without additional nonconforming modes, is used together with the eight-node hexahedron element with nonconforming modes in a mesh, there may be a significant inconsistency in the accuracy and thus in the error indicator during the adaptation process.

Therefore, to be consistent with the eight-node element with nonconforming modes in the accuracy, the proposed solid transition elements should also be improved by the means of addition of nonconforming displacement modes. In a similar way to the formulation for eight-node element(Cook 1981), the general displacement approximations for variable-node element with the modified nonconforming modes are of the form

$$u_e = \sum_{i=1}^{n} N_i(\xi, \eta, \zeta)\, u_i + \sum_{i=1}^{3} \tilde{N}_i(\xi, \eta, \zeta)\, \tilde{u}_i \tag{1}$$

where n is the number of nodes of the given element, N_i are the compatible interpolation functions given in Appendix, and $\tilde{N}_i$ are the corresponding nonconforming modes as follows;

$$\tilde{N}_1 = (1-\xi^2) - (\hat{N}_9 + \hat{N}_{11} + \hat{N}_{13} + \hat{N}_{15}) \tag{2.a}$$

$$\tilde{N}_2 = (1-\eta^2) - (\hat{N}_{10} + \hat{N}_{12} + \hat{N}_{14} + \hat{N}_{16}) \tag{2.b}$$

$$\tilde{N}_3 = (1-\zeta^2) - (\hat{N}_{17} + \hat{N}_{18} + \hat{N}_{19} + \hat{N}_{20}) \tag{2.c}$$

in which $\hat{N}_i$ are defined for different kinds of element types in Appendix and have nonzero values only when the corresponding node is assigned. This implies that, for example, if nodes 9 and 13 are assigned in the element, only $\hat{N}_9$ and $\hat{N}_{13}$ need to be defined in Eq. (2.a) for $\tilde{N}_1$. Thus the additional nonconforming displacement modes of variable-node elements are modified from those of the regular hexahedron element to consider the nature of variable nodes

that a transition element has.

The element strains ε are then given as

$$\varepsilon = \sum_{i=1}^{n} B_i \; u_i + \sum_{i=1}^{3} G_i \; \tilde{u}_i \tag{3}$$

where u_i and $\tilde{u}_i$ are nodal displacements and nonconforming interpolation parameters, respectively, and strain-displacement matrices B and G are obtained by differentiating the displacement shape functions N_i and $\tilde{N}_i$. Here, the following constraints should be imposed in order that the characteristics of the derivatives of the terms in the second parenthesis of Eq.(2) are consistent with those of the terms in the first parenthesis. For instance, as the derivatives of the terms in the first parenthesis $(1-\xi^2)$ with respect to η or ζ vanish, those of the second terms with respect to η or ζ should also vanish to eliminate the undesired effects. Thus

$$\frac{\partial \tilde{N}_1}{\partial \eta} = \frac{\partial \tilde{N}_1}{\partial \zeta} = 0 \qquad \frac{\partial \tilde{N}_2}{\partial \xi} = \frac{\partial \tilde{N}_2}{\partial \zeta} = 0 \qquad \frac{\partial \tilde{N}_3}{\partial \xi} = \frac{\partial \tilde{N}_3}{\partial \eta} = 0 \tag{4}$$

Then the strain energy of the proposed variable-node transition elements can be expressed by combining two parts as:

$$U = \frac{1}{2} \int_V \sigma^T B \, u \, dV + \frac{1}{2} \int_V \sigma^T B \, \tilde{u} \, dV \tag{5}$$

Extending the approach proposed for 8-node solid element by Wilson & Ibrahimbegovic (1990) to impose the requirement that under the state of constant stress, the srain energy associated with the incompatible modes vanishes:

$$\frac{1}{2} \sigma^T \int_V G \, dV \; \tilde{u} = 0 \tag{6}$$

Eq.(6) can be satisfied by adding a constant correction matrix G_c to the matrix G such that

$$\int_V \tilde{G} \, dV = \int_V (G + G_c) \, dV = 0, \tag{7}$$

and by the fact that G_c is a constant,

$$G_c = -\frac{1}{V} \int_V G \, dV \tag{8}$$

The correction matrix G_c can be evaluated numerically before the element stifness matrices are established. When element stiffnesses are evaluated, $\tilde{G}$ is used in stead of G at each integration point and the final stiffness matrix of transition element $\tilde{K}$ is constructed through the static condensation of the parts related to the additional nonconforming modes(Choi and Park 1989).

Numerical integration rule for variable-node transition elements

Transition elements can be classified into two types: the first type is used for connection of different order elements and the second is for connection of different layer patterns. While the

stiffness of the former type of a transition element can be computed by a normal Gaussian quadrature, the stiffness of the latter cannot be computed by applying the normal Gaussian integration rule over the entire domain ($-1 \leq \xi, \eta, \zeta \geq +1$) due to slope discontinuities at locations of irregular nodes. Thus, the stiffness matrices of the 3D solid transition elements for connection of different layer patterns can be obtained by the modified rule of Gaussian quadrature proposed by Gupta(1978) for 2D transition element which is applied independently to the three directions of natural coordinates ξ, η, and ζ.

3. Numerical tests for validation of the transition elements

Several numerical tests were carried out to evaluate the validity and performance of the proposed three-dimensional solid transition elements for the local refinement of 3D problems. Six different types of solid elements used for comparisons are designated as follows:

1. NC-V1 : the variable-node transition element with the modified nonconforming modes for the connection of different order elements,
2. NC-V2 : the variable-node transition element with the modified nonconforming modes for the connection of different layer patterns,
3. NC-8 : the regular eight-node solid element with the basic nonconforming modes and
4. C-V1, C-V2, and C-8 are elements corresponding to NC-V1, NC-V2 and NC-8 which do not have any nonconforming modes, respectively.

Test-1 : Eigenvalue analysis

To identify the possible spurious mechanisms, eigenvalue analyses of the individual element stiffness matrix were carried out for two types of transition solid elements with nonconforming modes. Since there are only six zero eigenvalues associated with rigid-body modes of a typical single unconstrained elements which are those with particular importance in the local mesh refinement as shown in Fig. 4, no spurious mechanisms were expected to develop in any of the transition solid elements presented in this study(see Table 1).

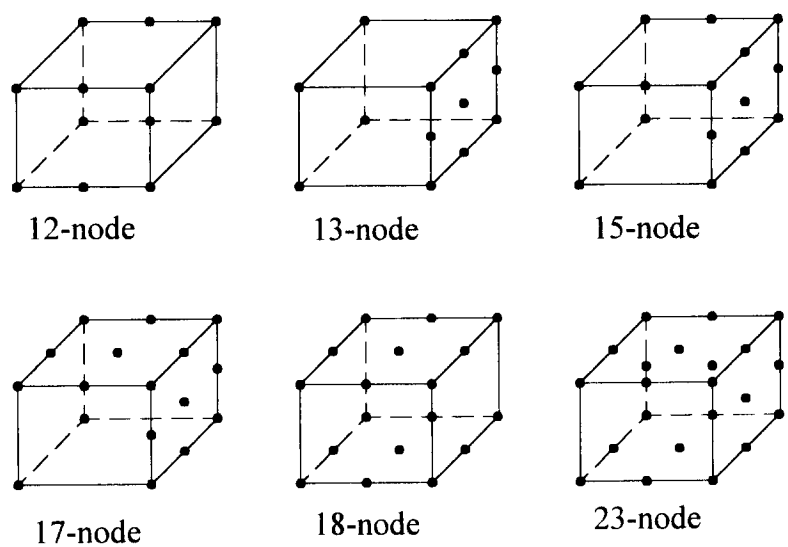

Fig. 4 Examples for typical transition elements

Table 1 Number of zero eigenvalues for single unconstrained transition elements with associated nonconforming modes (NC-V1 & NC-V2)

Typical Elements	Number of eigenvalues	Number of zero eigenvalues	Number of spurious zero-energy modes
12-node	36	6	0
13-node	39	6	0
15-node	45	6	0
17-node	51	6	0
18-node	54	6	0
23-node	69	6	0

Test-2 : Patch test

In order to check whether the proposed solid transition elements(NC-V1 & NC-V2) are capable of representing constant strain states, the patch test was carried out. The typical test model is shown in Fig. 5 which contains 12-node, 16-node and 17-node elements. Problem was solved with the prediscribed displacement boundary conditions and the obtained results which are identical with theoretical results for this problem are given in Table 2.

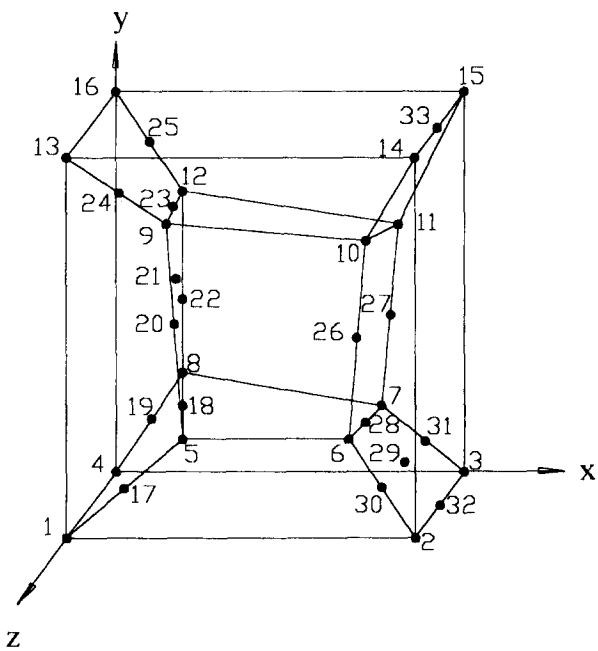

Note : Outer-dimensions are unit and coordinates of mid-edges of each element are the average value of both end nodes' coordinates of the corresponding edge

Coordinates of inner nodes

node	x	y	z
5	0.320	0.186	0.643
6	0.677	0.305	0.683
7	0.826	0.288	0.288
8	0.249	0.342	0.192
9	0.165	0.745	0.702
10	0.788	0.693	0.644
11	0.850	0.649	0.263
12	0.273	0.750	0.230

$E = 1.0 \times 10^6$
$v = 0.25$

Fig. 5 Patch test model for 3D solid

Table 2 Displacement boundary conditions and theoretical results

Boundary conditions	Theoretical solutions
$u = 10^{-3}(2x + y + z)/2$ $v = 10^{-3}(x + 2y + z)/2$ $w = 10^{-3}(x + y + 2z)/2$	$\varepsilon_x = \varepsilon_y = \varepsilon_z = r_{xy} = r_{yz} = r_{zx} = 10^{-3}$ $\sigma_x = \sigma_y = \sigma_z = 2000$ $\tau_{xy} = \tau_{yz} = \tau_{zx} = 400$

Test-3 : Cantilever beam

To verify the performance of the new transition element and its applicability to the adaptive mesh refinement, a cantilever beam acted upon by two load cases, i.e. shear forces and pure bending at tip was tested (see Fig. 6). The test meshes which are composed of various transition elements are shown in Fig. 7. The vertical displacement at A and the bending stress at B for various combinations of transition elements are presented in Table 3 and 4 along with the exact solutions(Roark 1965) for the comparison. Here, it is shown that the proposed nonconforming transition solid elements(NC-V1, NC-V2) give superior results over the conventional element for regular mesh shapes. In cases of highly distorted meshes, the accuracies of results obtained by using elements with nonconforming modes are still markedly better than those obtained by the conventional elements. It is noted through the numerical test results for the case of distorted meshes that the mesh gradation by transition elements is needed to maintain the mesh regularity which is greatly important for the accuracy of the results.

Test-4 : Boussinesq problem

This example is selected to demonstrate the effectiveness of transition element for local mesh refinement. This is especially to show that when the transition elements are used in modelling, the total degrees of freedom can be markedly reduced and the similar results to or the superior results than those by a single 8-node element can be obtained. To model one quadrant of the semi-infinite body of the Boussinesq problem(see Fig. 8), two kinds of meshes are used. Fig. 8(c) shows the mesh which uses the proposed transition elements(NC-V2) at the transition zones between fine elements and coarse elements. The mesh shown in Fig. 8(d) is composed of 8-node solid elements only and solutions with this mesh are obtained by using SAP90 program(Wilson, E.L. and Habibullah A. 1989).

By comparison of total degrees of fredom(DOF) of two models, the number of DOF of the former mesh is 657 and that of the latter mesh is 931. A more refined mesh(Fig. 8(e)) of 1062 DOF is additionally constructed to validate the effectiveness and applicability of the proposed transition elements to the adaptive mesh refinement. The bottom surface is completely fixed. Two Planes, $x=0$ and $y=0$, are constrained so as to properly represent the symmetry about $x=0$ and $y=0$. The applied load is P=10,000lb. The results for each mesh are shown in Table 5 and Table 6 and the exact values are calculated by Boussinesq's formular(Timoshenko and Goodier 1970). It is especially noticed from analysis results for Mesh-3 that the mesh at the area having the steep stress gradient can be efficiently graded by using the proposed transition elements and with a minimum number of additional degrees of freedom, the superior results at the detailed intrested area can be also obtained.

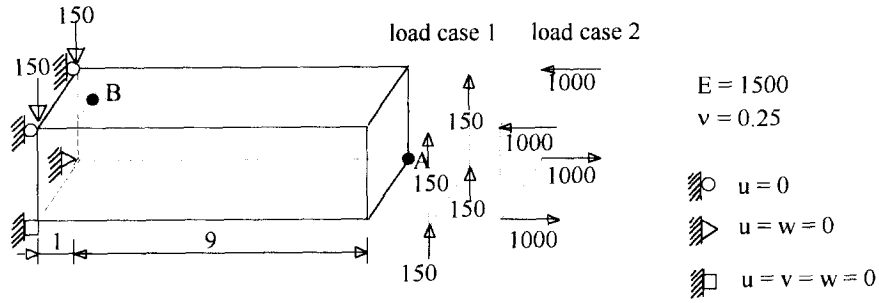

Fig. 6 Schematic model

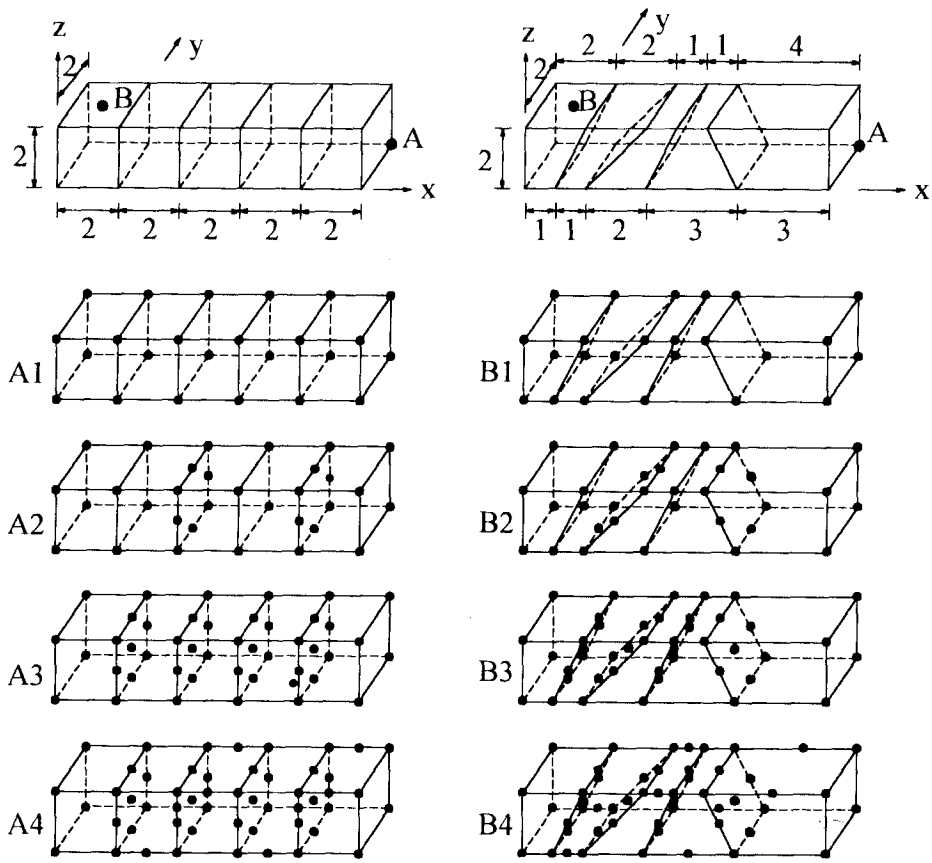

(a) Regular meshes (b) General meshes

Fig. 7 Test meshes of variable transition elememts

Table 3(a) Vertical displacement at point A of regular meshes

	Load Case 1			Load Case 2		
Mesh type	C-V1	NC-V1	NC-V2	C-V1	NC-V1	NC-V2
A1	68.45	101.40	101.40	66.67	100.00	100.00
A2	70.10	100.96	100.67	68.86	99.43	99.09
A3	72.33	101.28	100.08	70.83	99.97	98.51
A4	78.48	100.27	98.99	77.86	98.07	97.00
Exact		102.60			100.0	

Table 3(b) Stress σt_{xx} at point B of regular meshes

	Load Case 1			Load Case 2		
Mesh type	C-V1	NC-V1	NC-V2	C-V1	NC-V1	NC-V2
A1	−2972.0	−4050.0	−4050.0	−2200.0	−3000.0	−3000.0
A2	−2972.0	−4050.0	−4050.0	−2200.0	−3000.0	−3000.0
A3	−2936.0	−4063.0	−4063.0	−2167.0	−3005.0	−3007.0
A4	−3001.0	−3968.0	−3968.0	−2241.0	−2905.0	−2986.0
Exact		−4050.0			−3000.0	

Table 4(a) Vertical displacement at point A of general meshes

	Load Case 1			Load Case 2		
Mesh type	C-V1	NC-V1	NC-V2	C-V1	NC-V1	NC-V2
B1	49.33	89.89	89.89	44.38	87.45	87.45
B2	56.38	86.66	83.90	51.59	83.46	80.50
B3	64.61	89.57	78.84	58.42	86.03	75.85
B4	79.49	97.40	82.66	78.60	95.99	82.09
Exact		102.60			100.0	

Table 4(b) Stress sxx at point B of general meshes

	Load Case 1			Load Case 2		
Mesh type	C-V1	NC-V1	NC-V2	C-V1	NC-V1	NC-V2
B1	−2415.0	−3097.0	−3097.0	−1736.0	−2262.0	−2262.0
B2	−2420.0	−3103.0	−3097.0	−1757.0	−2286.0	−2277.0
B3	−3129.0	−4018.0	−3622.0	−2300.0	−3002.0	−2672.0
B4	−3338.0	−3959.0	−3611.0	−2460.0	−2908.0	−2652.0
Exact		−4050.0			−3000.0	

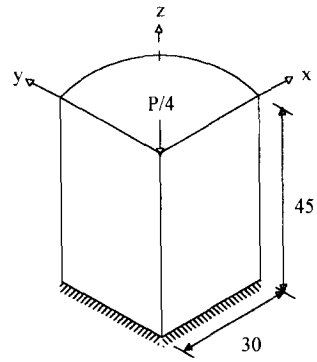

$E = 1.0 \times 10^6$ psi
$\nu = 0.3$
P = 10000 lb

(a) Schematic model

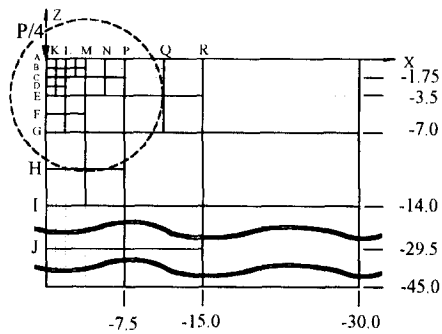

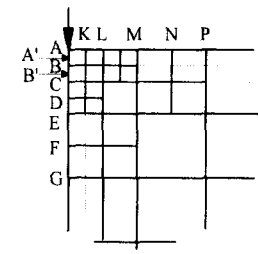

Details in the dashed circle

(b) Side view of meshes

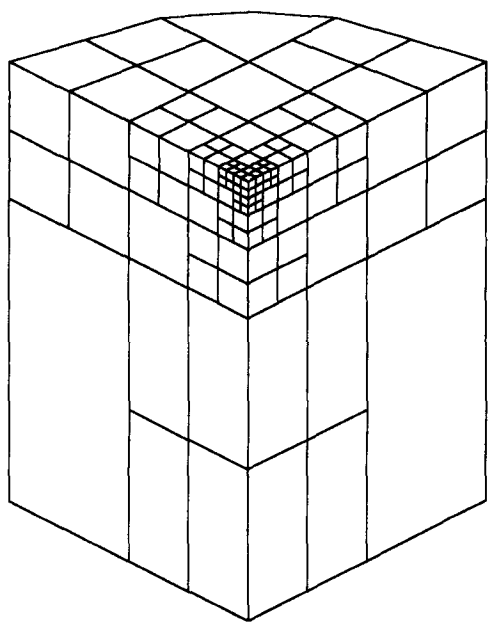

(c) Mesh-1 with transition elements
(total DOF = 657)

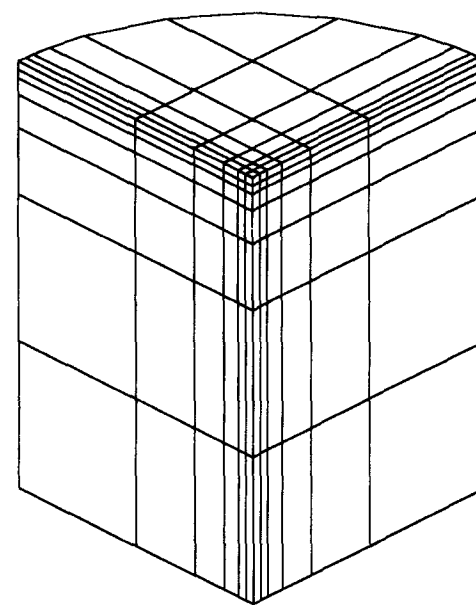

(d) Mesh-2 with 8-node elements
(total DOF = 931)

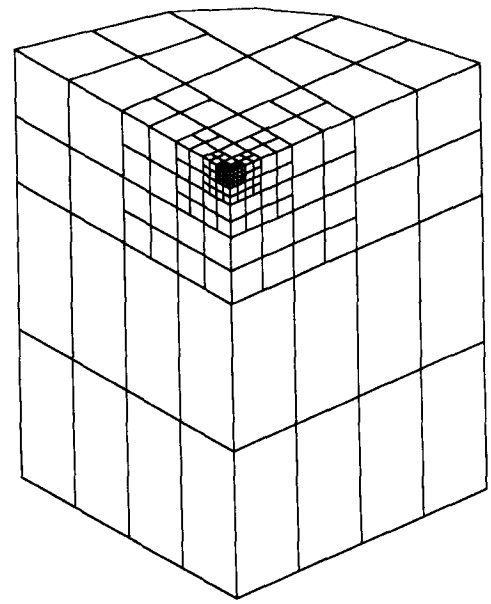

(e) Mesh-3 with transition elements
(total DOF = 1062)

Fig. 8 One quadrant of semi-infinite body

Table 5 Z-direction displacements(in $\times 10^{-5}$)

Mesh	along z-axis					along x-axis			
type	A	B	C	E	G	L	M	P	R
Mesh-1	182.70	53.15	24.32	12.59	5.72	14.57	6.29	3.09	1.34
Mesh-2	183.31	53.60	24.64	12.97	6.20	15.41	6.90	3.18	1.41
Mesh-3	367.33	50.04	26.73	13.20	6.29	14.45	6.96	3.26	1.45
Exact	∞	56.75	28.38	14.19	7.09	15.45	7.72	3.86	1.93

Table 6(a) Normal stress σ_z (psi) for Mesh-1

	AB	BC	CE	EG	GI
Mesh-1	-17940.	-3291.	-665.0	-185.9	-40.9
Exact	-24945.	-2771.	-692.9	-173.2	-43.3

Table 6(b) Normal stress σ_z (psi) for Mesh-2

	AB	BC	CD	DE	EF	FG	GH	HI
Mesh-2	-17970.	-3296.	-789.6	-512.2	-238.4	-134.1	-62.0	-33.2
Exact	-24945.	-2771.	-997.8	-509.1	-249.5	-127.3	-62.4	-31.8

Table 6(c) Normal stress σ_z (psi) for Mesh-3

	AA′	A′B	BB′	B′C	CD
Mesh-3	-71840.	-13130.	-3181.0	-2037.0	-955.9
Exact	-99780.	-11078.	-3989.4	-2035.7	-997.8
	DE	EF	FG	GH	HI
Mesh-3	-537.8	-246.1	-135.0	-62.1	-33.5
Exact	-509.1	-249.5	-127.3	-62.4	-31.8

4. Conclusions

A new solid elements are established to be used effectively as transition elements in three-dimensional modelling. A series of 3-D transition elements are systematically developed through addition of variable nodes(irregular nodes) to the basic 8-node element as needed and selection of the shape functions to connect the refined regions and unrefined regions. This element was improved by the addition of the modified nonconforming modes.

From the numerical tests, it was verified that the proposed elements passed patch tests and there are no zero energy mechanisms identified by the eigen value analysis in the elements. The improvement achieved by the addition of the nonconforming modes associated with variable nodes was significant making the use of this type of element in modelling transition zone very effective and stable. It is also demonstrated from numerical tests that the proposed elements can be effectively used for local mesh refinement without imposing any displacement constraints which are necessary to guarantee the interelement compatibility with the neighbored eight-node elements generated by the subdivision. Furthermore, the introduction of the transition elements makes it possible to construct meshes without distortions which may have a negative effect on the accuracy of analysis results.

References

Chang, K.H. and Choi, K.K. (1992), "An error analysis and mesh adaptation method for shape design of structural components", *Comp. and Struct.*,44(6), 1275-1289.

Choi, C.K. and Lee, N.H. (1993), "A 3-D adaptive mesh refinement using variable-node solid elements with nonconforming modes", *Proceedings of Second Asian-Pacific Conference on Computational Mechanics*, Sydney, Austrailia, August.

Choi, C.K. and Park, Y.M. (1989), "Nonconforming transition plate bending elements with variable mid-side nodes", *Comp. and Struct.*, 32(2), 295-304.

Cook, R.D.(1981), *Concepts and Applications of Finite Element Analysis*, 2nd edn., Jhon Wiley & Sons, New York.

Devloo, P.R. (1991), "A three-dimensional adaptive finite element strategy", *Comp. and Struct.*, 38(2), 121-130.

Gupta, A.K. (1978), "A finite element for transition from a fine to a coarse grid", *Int. J. Num. Meth. Eng.*, 12(1), 35-45.

Roark, R.J. (1965), *Formulas for Stress and Strain*, McGraw-Hill, 4th edn., New York, 104-106.

Timoshenko, S.P. and Goodier, J.N. (1970), *Theory of Elasticity*, McGraw-Hill, 3rd edn., New York, 398-402.

Wilson, E.L. and Habibullah A. (1989), SAP90-A Series of Computer Programs for the Static and Dynamic

Finite Element Analysis of Structures, Computers and Structures, Inc., Berkeley, California.
Wilson, E.L. and Ibrahimbegovic A. (1990), "Use of incompatible displacement modes for the calculation of element stiffnesses or stresses", *Finite Element in Analysis and Design* 7, 229–241.
Zienkiewicz, O.C. and Taylor, R.L. (1989), *The Finite Element Method, McGraw-Hill,* 4th edn., 1, London.

Appendix

This appendix shows only the simple descriptions of shape functions for 8-to-27 variable-node solid transition elements. It is to be noted that the derived shape functions N_9 to N_{27} have nonzero values only when the corresponding middle nodes are assigned.

The shape functions for the eight corner nodes 1 through 8 are modified by the addition of irregular nodes as follows:

$$N_1 = \hat{N}_1 - 1/2(N_9 + N_{12} + N_{17}) - 1/8\ N_{21} - 1/4(N_{22} + N_{25} + N_{26})$$
$$N_2 = \hat{N}_2 - 1/2(N_9 + N_{10} + N_{18}) - 1/8\ N_{21} - 1/4(N_{22} + N_{23} + N_{26})$$
$$N_3 = \hat{N}_3 - 1/2(N_{10} + N_{11} + N_{19}) - 1/8\ N_{21} - 1/4(N_{23} + N_{24} + N_{26})$$
$$N_4 = \hat{N}_4 - 1/2(N_{11} + N_{12} + N_{20}) - 1/8\ N_{21} - 1/4(N_{24} + N_{25} + N_{26})$$
$$N_5 = \hat{N}_5 - 1/2(N_{13} + N_{16} + N_{17}) - 1/8\ N_{21} - 1/4(N_{22} + N_{25} + N_{27})$$
$$N_6 = \hat{N}_6 - 1/2(N_{13} + N_{14} + N_{18}) - 1/8\ N_{21} - 1/4(N_{22} + N_{23} + N_{27})$$
$$N_7 = \hat{N}_7 - 1/2(N_{14} + N_{15} + N_{19}) - 1/8\ N_{21} - 1/4(N_{23} + N_{24} + N_{27})$$
$$N_8 = \hat{N}_8 - 1/2(N_{15} + N_{16} + N_{20}) - 1/8\ N_{21} - 1/4(N_{24} + N_{25} + N_{27})$$

The shape functions for mid-edge nodes 9 through 20 are also modified by the addition of a centroid node 21 and the mid-face nodes 22 through 27 as:

$$N_i = \hat{N}_i - 1/4\ N_{21} + 1/2(N_a + N_b) \qquad \text{for } i = 9 \text{ to } 20$$

Here, nodes *a* and *b* are those at centroid of two faces sharing node i respectively. That is, nodes a and b based on the basic configuration shown in Fig. 2 are as:

$a = i+13$ and $b = 26$ for $i = 9$ to 12; $a = i+9$ and $b = 27$ for $i = 13$ to 16; $a = 22$ and $b = 26$ for $i = 17$; $a = i+4$ and $b = i+5$ for $i = 18$ to 20.

The shape functions associated with node 21 at centroid of hexahedron and node 22 through 27 at center of faces are constructed as follows:

$$N_{21} = \hat{N}_{21} \qquad \text{for node 21}$$
$$N_i = \hat{N}_i - 1/2\ N_{21} \qquad \text{for node 22 through 27}$$

where, for element NC-V2

$$\hat{N}_i = 1/8(1+\xi\xi_i)(1+\eta\eta_i)(1+\zeta\zeta_i) \qquad \text{for } i = 1 \text{ to } 8$$
$$\hat{N}_i = 1/4(1-|\xi|)(1+\eta\eta_i)(1+\zeta\zeta_i) \qquad \text{for } i = 9 \text{ to } 15$$
$$\hat{N}_i = 1/4(1+\xi\xi_i)(1+|\eta|)(1+\zeta\zeta_i) \qquad \text{for } i = 10 \text{ to } 16$$
$$\hat{N}_i = 1/4(1+\xi\xi_i)(1+\eta\eta_i)(1+|\zeta|) \qquad \text{for } i = 17 \text{ to } 20$$
$$\hat{N}_i = (1-|\xi|)(1-|\eta|)(1-|\zeta|) \qquad \text{for } i = 21$$
$$\hat{N}_i = 1/2(1-|\zeta|)(1+\eta\eta_i)(1-|\zeta|) \qquad \text{for } i = 22 \text{ to } 24$$
$$\hat{N}_i = 1/2(1-\xi\xi_i)(1-|\eta|)(1-|\zeta|) \qquad \text{for } i = 23 \text{ to } 25$$
$$\hat{N}_i = 1/2(1-|\xi|)(1-|\eta|)(1-\zeta\zeta_i) \qquad \text{for } i = 26 \text{ to } 27$$

and for element NC-V1, $|\xi|$, $|\eta|$, and $|\zeta|$ in the above shape functions are just replaced to ξ^2, η^2, and ζ^2 respectively.